receives signal from more number of satellites of the GPS satellite constellation [Pathak *et al.* (2003)], [Agarwal *et al.* (2013)]. It is more convenient to design a simple linearly polarized antenna rather than a more complex and expensive circularly polarized one. A number of PIFA structures have been developed for this purpose [Pathak *et al.* (2003)], [Agarwal *et al.* (2013), Tan (2004), Serra *et al.* (2010)].

Unfortunately, these antennas have not been evaluated in an array environment for MIMO applications. Also the footprints of these multiband antenna elements make them less attractive for mobile phones. To the best of the knowledge little work has been carried out on the MIMO antenna which incorporates GPS application with other communication bands [Park *et al.* (2009a), Park *et al.* (2009b), Wang *et al.* (2010), Glogowski and Peixeiro (2008)]. Park *et al.* [Park *et al.* (2009a)] proposed two different monopole antenna elements for quad band applications whereas in [Park *et al.* (2009b), Wang *et al.* (2010)], design of dual feed multiband monopole antenna is proposed. Unfortunately, [Wang *et al.* (2010), Glogowski and Peixeiro (2008)] have not evaluated antenna performance in the array environment. In [Glogowski and Peixeiro (2008)], MIMO antenna consisting of two PIFA and five inverted-F antennas which covers GSM1800, UMTS, IEEE 802.11b, Bluetooth and GPS bands is reported. More number of antenna elements used for various applications increases the system complexity. Therefore, it is highly desirable to design new multiband antenna that could be easily integrated as array into MIMO enabled multi-standard mobile phones.

After, integration of antenna with the mobile devices, the study of interaction between mobile phone and user body is also an important factor. However, the amount of power received from mobile base station to mobile user depends on other factor of mobile phone and antenna design. Moreover, mobile phone generally used in close proximity of user's body, which reduces received power at the mobile terminal. The body loss (ratio of efficiency with and without user body) is significantly depends on the design of the antenna for mobile phones. The antenna characteristics, such as impedance matching, radiation efficiency, and radiation pattern are affected by the presence of the objects, especially

presence of user in the vicinity of the antenna. With an increase in the number of applications and the functions required for these applications, the interaction between the mobile phone antenna and the surrounding components is inevitable. Given the real-estate limitation and the requirement that the antenna be of low profile, realization of good impedance matching over multiple bands is indeed very challenging for the antenna designers.

Some of the mobile terminal antennas have been studied in the presence of human head and hand [Gao *et al.* (2013). Yu *et al.* (2010), Pelosi *et al.* (2010), Iivonen *et al.* (2011), Holopainen *et al.* (2011), Li *et al.* (2009)]. Unfortunately, researchers in [Gao *et al.* (2013). Yu *et al.* (2010), Pelosi *et al.* (2010), Iivonen *et al.* (2011), Holopainen *et al.* (2011), Li *et al.* (2009)], focused only on the user effects on a single antenna element whereas, in next generation mobile phones, the multi antenna system with MIMO implementation is more demanding. So in view of this, we can not conclude the effect of user on the diversity performances with the single antenna elements. Further, diversity antennas are proposed by some of the authors along with the performance study in user proximity [Plicaic *et al.* (2008), Buskgaard *et al.* (2014), Zhang *et al.* (2013), Plicanic *et al.* (2009)].

In this chapter, a quad-band antenna array consisting of two PIFA elements for MIMO application is presented. The proposed antenna operates over LTE2500 and GPS L1 along with other mobile communication bands. Since, for the fourth generation mobile terminals having high data rate LTE band need to be covered, therefore, the proposed antenna covers one of the LTE2500 band which makes it suitable for the fourth generation (4G) terminals. The proposed antenna occupies a volume of $25 \times 10 \times 5.8$ mm^3 above the mobile circuit board and is suitable to be fabricated at low cost and attractive for next generation mobile phones. The two antenna elements are separated by a distance of 40 mm at the ground plane, providing good isolation (better than -15 dB) and low correlation coefficient (less than 0.015) between the antenna elements. Further, the effect of user body on the performance of quad-band MIMO antenna is studied by considering the three different commonly used configurations namely, SAM head and PDA hand (Talk mode), PDA hand (Data mode), and Dual hand (Read mode). The *S*-parameters,

diversity parameters, SAR to PEAK Location Spacing Ratio (SPLSR), and Total Radiated Power (TRP) are calculated in the user proximity.

5.2 Antenna Configuration and Design

The configuration along with the fabricated prototype of the proposed antenna for MIMO application is shown in Fig. 5.1. The two antenna elements referred as Antenna 1 and Antenna 2 are mirror image of each other, and are mounted at the top corners of mobile circuit board. FR4 substrate (ε_r = 4.4) of 100 × 60 × 0.8 mm^3 is used as the mobile circuit board which is having ground plane etched at its bottom side.

Fig. 5.2(a) shows the 3D view of the proposed antenna. The unfolded view of the main radiator and added resonating arm are shown in Fig. 5.2(b) and (c). It can be seen that a circle of radius r (r > radius of coaxial cable) is cut at the folded patch to avoid the short-circuiting of coaxial cable with the folded patch. Each antenna element of MIMO configuration is with an air gap of 5 mm above the ground plane and is connected to the ground plane via a shorting plate. The antenna is basically designed for 1.575 GHz using the Eq. (5.1) [Ogawa and Uwano (1994)],

$$f = \frac{c}{4(L+W)} \tag{5.1}$$

where, c is speed of light, L and W are the length and width of the rectangular PIFA, respectively, and f is the resonant frequency.

The dimensions of PIFA are calculated by using Eq. (5.1) by fixing one of the dimensions say width, which is small enough to get higher separation between two antenna elements. Therefore, the length of the PIFA becomes large to be integrated within the small space of mobile phones. Thus we folded the structure and etched it over the FR4 substrate of 0.8 mm thickness and it is referred as Configuration 1 during evolution of antenna elements. It can be seen that the top patch of the radiator is fed by a coaxial cable at (x, y) = (10 mm, 2 mm) which is shown in Fig. 5.2. Feed position is optimized to get the better impedance

matching. The patch gives the desired resonance at 1.575 GHz along with the one higher order mode centered at 3.1 GHz. Another higher order mode appeared at 5.1 GHz, but with a reflection coefficient not better than - 6 dB as shown in Fig. 5.3. This resonating mode does not have proper impedance matching ($S_{11} = -5.18$ dB). Impedance characteristics of higher mode can be improved by either tuning the feeding position or adding matching circuit. Other modes may get affected if tuning of the feeding position is applied for improvement. Therefore, another technique of cutting a rectangular slot of size 12.3×1 mm^2 is applied which may work similar to the matching circuit for the improvement of the characteristics of the higher order mode. This mode starts resonating at 5.25 GHz with S_{11} value of -19.5 dB, which can be utilized for HiperLAN1 application as shown in Fig. 5.3. Also, it can be observed that the cutting of the slot in the PIFA does not affect the characteristics of lower resonating modes. The slot on top surface of the PIFA geometry is referred as Configuration 2.The working of the slot can be understood by the current distribution plot as shown in Fig. 5.4. It can be observed from current distribution plot at 5.25 GHz that the antenna appears to work in $\lambda/2$ resonant mode antenna, taking into account the orientation of current distribution as seen on the top and opposite surfaces of the PIFA. Now, for further introduction of resonance at the center frequency of LTE2500 band, a resonating copper arm is introduced into the structure which consists of a rectangular vertical strip and inverted L-shaped horizontal strip, referred as proposed structure. The vertical strip provides the inductive effect and is connected to the edge of the lower patch of the main radiator. The overall size of each antenna element is 25×10 mm^2. Fig. 5.3 shows the effect of added extra resonating arm into the antenna structure. It is observed that in the absence of this arm, antenna is having triple band behavior with a second band from 2.53 GHz to 3.43 GHz. This second band is having 600 MHz of bandwidth (2.7 GHz to 3.3 GHz) which is not used in any communication applications. Thus to make best use of this band, a resonating arm is added that provides dual band characteristics with the frequency ranges from 2.39 GHz to 2.77 GHz and 3.09 GHz to 3.47 GHz which can be used for Wi-Fi/Bluetooth, LTE2500, and WiMAX applications, respectively as shown in

Fig. 5.3. This arm is having quarter wavelength operation and is transformed into L-shape to maintain small size of the antenna.

5.3 Results and Discussion

All the simulations are carried out done on Ansoft's HFSS simulation software. Further, CST MWS is used to verify the HFSS result before going for the fabrication of the antenna and also used to calculate the radiation and diversity performances of the MIMO antenna.

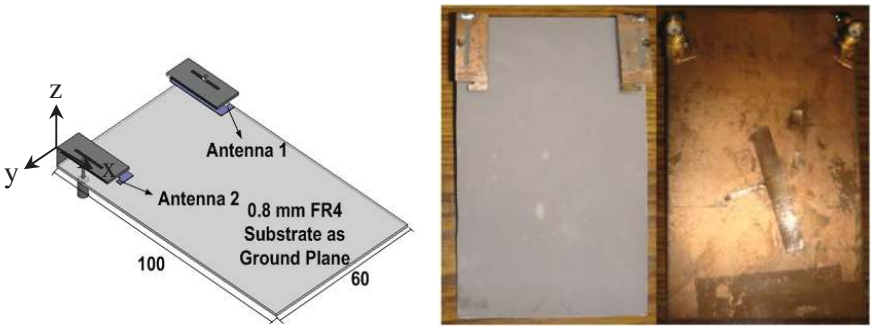

Figure 5.1: Configuration of proposed antenna with fabricated prototype.

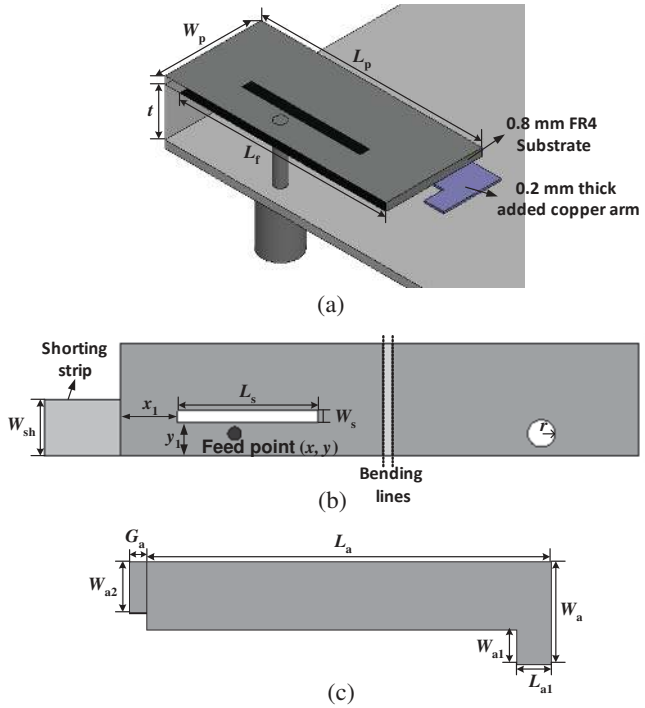

Figure 5.2: (a) 3-D view of the single antenna element, (b) Detailed dimension of proposed patch unfolded into a planar structure, and (c) Detailed dimension of added resonating arm.

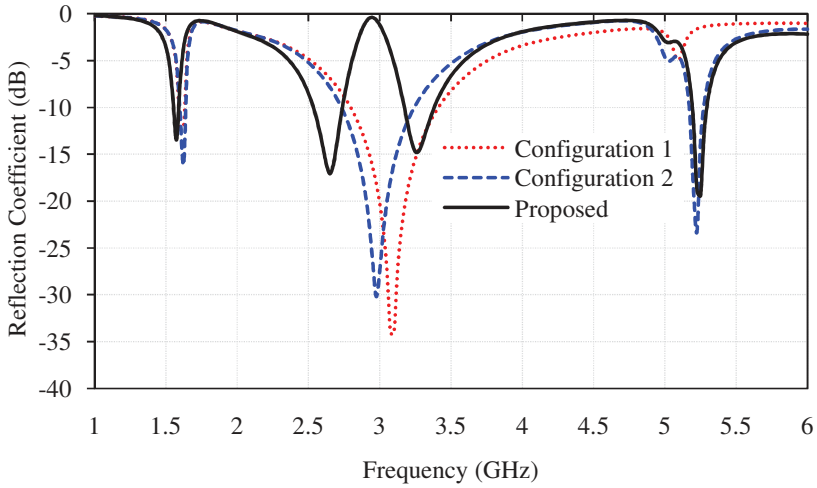

Figure 5.3: Evolution of antenna element and respective reflection coefficient.

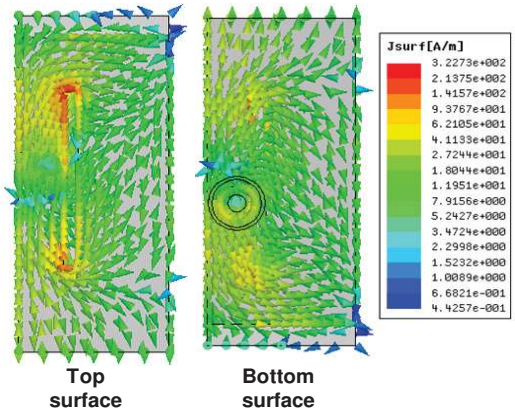

Figure 5.4: Surface current distribution on the antenna at 5.25 GHz.

5.3.1 *S*-parameters and Radiation Performances

5.3.1.1 Parametric Analysis

Parametric investigations of some key parameters are carried out to analyze their effects on antenna reflection and coupling *S*-parameters using Ansoft's HFSS software.

In view of this, slot which is created on the top of the folded patch is optimized to get desired resonance frequency band. Position of slot (x_1, y_1) from edges of the patch and width of slot (W_s) are optimized for better impedance matching at higher frequency side. The variation of x_1, y_1, and W_s are shown in Fig. 5.5(a), (b), and (c). It is observed that all the dimensions of slot are affecting only higher frequency band (5.25 GHz), because it is used to improve the impedance

matching at higher frequency band as discussed in earlier section. When x_1 increases, 5.25 GHz resonant frequency increases toward higher frequency side. The optimum frequency band is achieved for a particular value of x_1 = 5 mm. The position of slot from feed position is very sensitive for 2.25 GHz resonance. When slot moves either far from feed point or moves near to the feed point, the impedance matching is deteriorated. The optimum distance of slot from edge of the substrate is 3mm. In addition to the position of slot, width of slot is also optimized for proper tuning of the higher frequency band. The optimized value of slot width is 1mm. All these parameters are not affecting the coupling parameters of the proposed antenna.

Further, shape parameters of the added resonating arm are optimized to tune the frequency bands at 2.62 GHz and 3.35 GHz. This resonating arm is added to obtained Wi-Fi, LTE2500, and WiMAX frequency bands, so the effect of shape parameters of the added resonating arm is on these operating bands only. In order to observe this, parameters G_a, L_a, W_{a1}, W_{a2}, and W_{sh} are tuned and results are shown in Fig. 5.6 and Fig. 5.7. The effect of G_a is shown in Fig. 5.6(a). It is observed that as G_a increases, resonance at 2.62 GHz shifts towards lower frequency side and simultaneously bandwidth is reduced whereas bandwidth of 3.35 GHz band gets enhanced. By the trade-off between impedance matching and bandwidth the optimized value of G_a is 1mm. Similarly, length of the added resonating arm L_a and W_{a1} are optimized and same trend is observed as observed in case of G_a and results are shown in Fig. 5.6(b) and (c). The variations of W_{a2} are shown in Fig. 5.7(a). It is observed that as W_{a2} increases, resonance frequency of 2.62 GHz and 3.35 GHz bands shifts toward higher frequency side whereas other operating bands are not affected. The optimized value of W_{a2} is 3mm. Due to all above parameters, the isolation between two antenna is not disturbed and remains below -12dB over all the operating frequency bands. Further, width of shorting strip W_{sh} is tuned and shown in Fig. 5.7 (b). As W_{sh} increases, resonant frequency at 2.62 GHz shifts towards higher frequency side and all other bands remains unaffected. All the optimized values of the shape parameters are given in the Table 5.1.

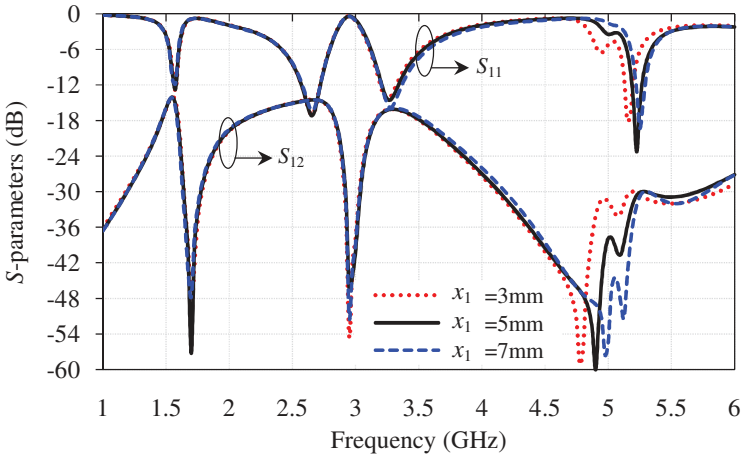

(a)

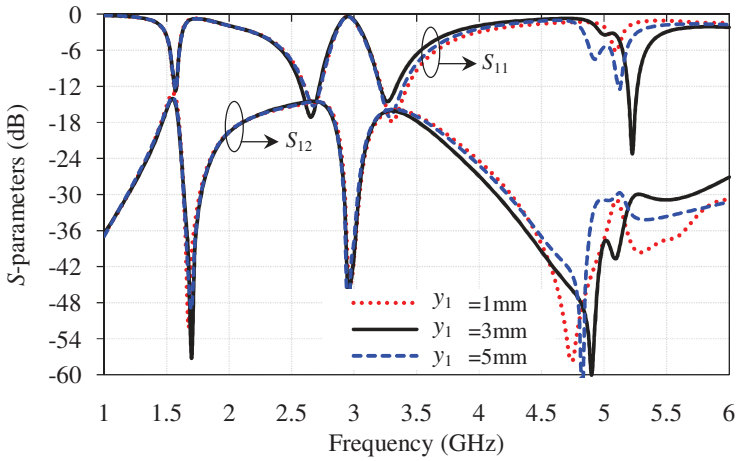

(b)

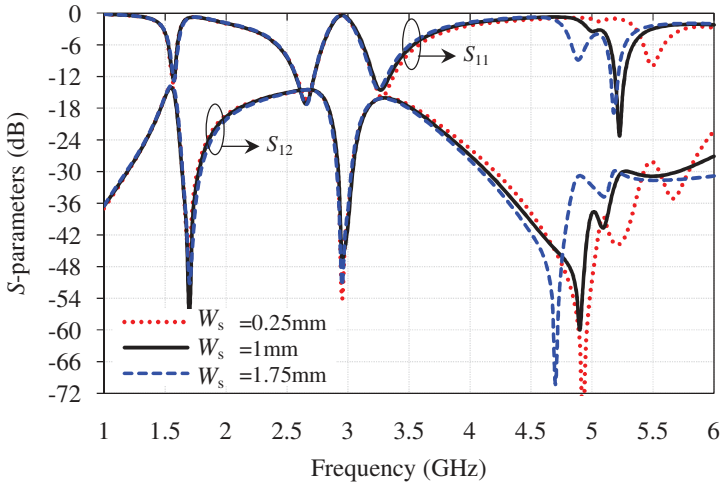

(c)

Figure 5.5: Variations of *S*-parameters with slot shape parameters, (a) x_1, (b) y_1, and (c) W_s.

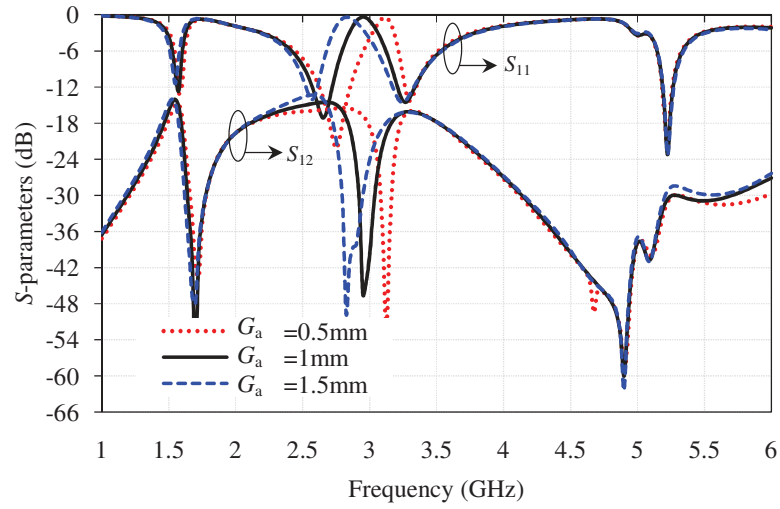

(a)

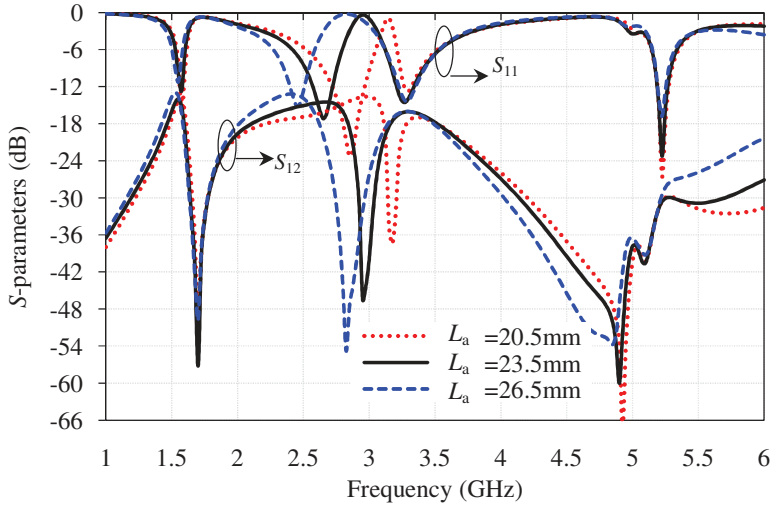

(b)

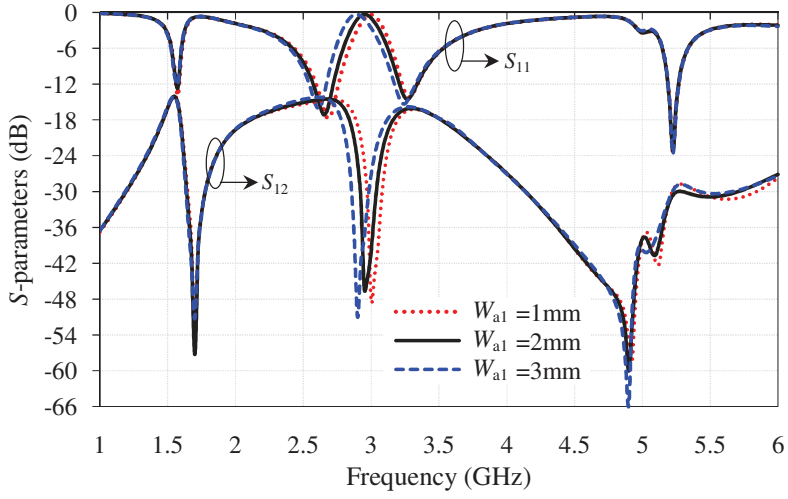

(c)

Figure 5.6: Variation of *S*-parameters with antenna shape parameters, (a) G_a, (b) L_a, and (c) W_{a1}.

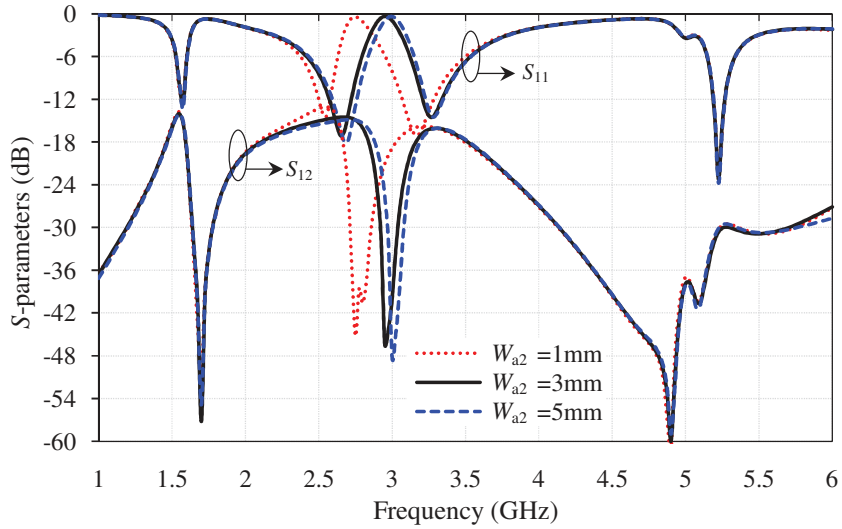

(a)

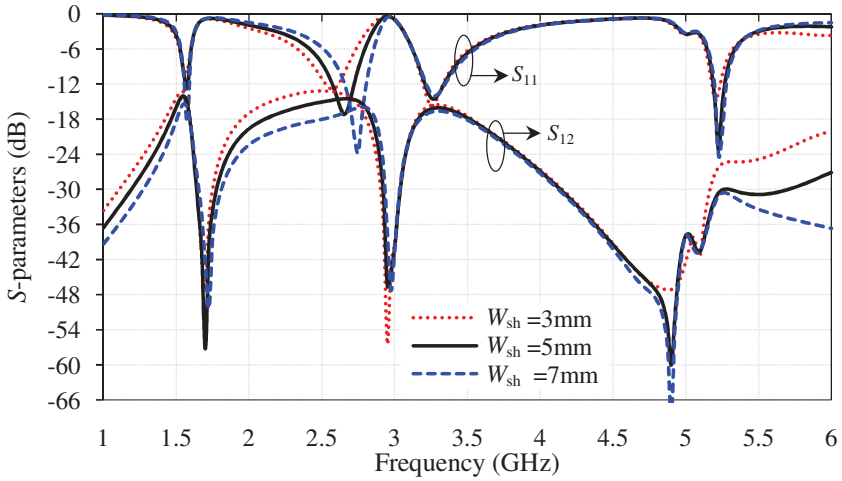

(b)

Figure 5.7: Variation of *S*-parameters with antenna shape parameters, (a) W_{a2} and (b) W_{sh}.

5.3.1.2 Simulated and Measured *S*-parameters

The antenna is designed to cover GPS L1 (1.565-1.585 GHz), Bluetooth/Wi-Fi (2.4-2.484 GHz), LTE2500 (2.5-2.57 GHz for uplink, 2.62-2.69 GHz for downlink), WiMAX (3.1-3.5 GHz), and HiperLAN1 (5.15-5.35 GHz) bands. The antenna is optimized to obtain minimum reflection and high isolation between the two antenna elements. The simulated and measured S_{11} and S_{21} parameters of the proposed antenna are shown in Fig. 5.8. It is observed that the results of the HFSS

and CST MWS simulations are in good agreement. The measured S_{11} results are deviated from the simulated results but are covering the frequency bands of interest. The measured S_{21} results are getting improved and isolation is better than -15 dB in all the bands. The deviation in the measured and simulated results may be due to the manufacturing tolerances, tolerances of adjusting the gap between the radiators and the ground plane, and interference of the surrounding objects during the measurement.

Table 5.1: Optimized shape parameters of the proposed antenna.

Parameter	Value (mm)	Parameter	Value (mm)
L_p	23	W_a	6
W_p	10	G_a	1
L_f	21.5	L_{a1}	2
t	5	W_{a1}	2
L_s	12.3	W_{a2}	3
W_s	1	x_1	5
W_{sh}	5	y_1	3
L_a	23.5	(x, y)	(10, 2)

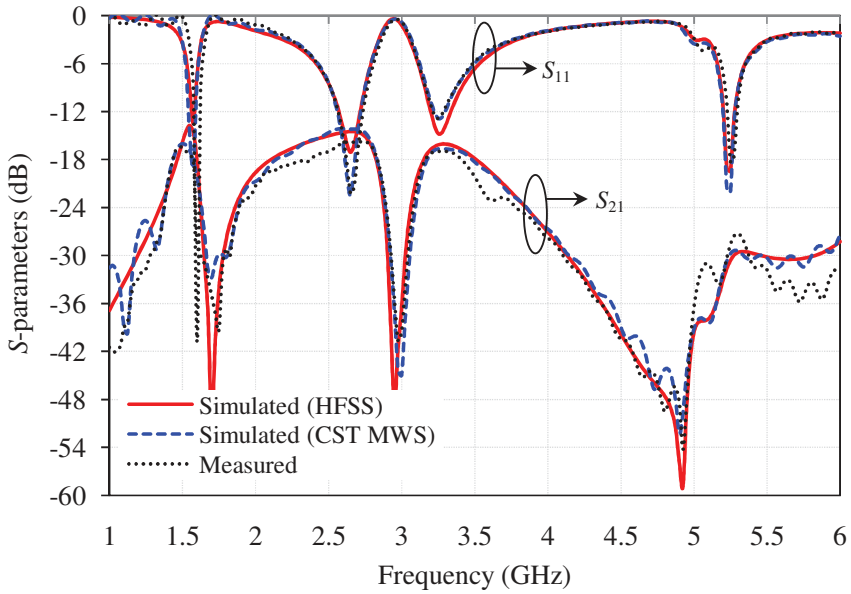

Figure 5.8: *S*-parameters of the proposed MIMO antenna.

5.3.1.3 Radiation Performances

The simulated 3D far-field radiation patterns and measured 2D radiation patterns of the proposed quad-band MIMO antenna are shown in Fig. 5.9. In the case of MIMO antenna system only one port is excited while keeping other port matched terminated with 50Ω load. The radiation patterns of Antenna 1 and Antenna 2 are almost mirror images of each other over all the operating frequency bands. That means they are covering the complementary space regions and indicating that the proposed MIMO antenna has good pattern diversity characteristics.

In this structure, the total antenna efficiency is calculated by considering the mismatch losses. The plots of total efficiency and gain at port 1 of MIMO antenna are plotted in Fig. 5.10, that are taken from CST MWS. The total efficiency lies between 33% to 40% in GPS L1 band, 93% to 96% in Wi-Fi and LTE2500 band, 96% to 97% in WiMAX band, and 40% to 75% in HiperLAN1 band whereas the measured peak realized gain varies between -2 to 0 dBi in GPS L1 band, 2.3 to 4.5 dBi in Wi-Fi and LTE2500 band, 4 to 4.3dBi in WiMAX band, and 0 to 2 dBi in HiperLAN1 band.

5.3.2 Diversity Parameters Analysis in Free Space

The diversity parameters are studied to characterize the proposed quad-band diversity antenna. All the diversity parameters such as ECC, MEG, and EDG are studied with CST MWS to check the diversity performances of the proposed MIMO antenna.

5.3.2.1 Envelope Correlation Coefficient (ECC)

For evaluating the diversity capability of the MIMO antenna, correlation between two antenna elements is taken into consideration. The correlation coefficient can be calculated using far field radiation pattern data as calculated in previous chapters by considering the antenna system as lossy structure and in scattering environment. Fig. 5.11 shows the simulated results of ECC with respect to frequency. It can be observed that the ECC values are less than 0.1 for the desired bands, which is well within the maximum allowed limit of ECC.

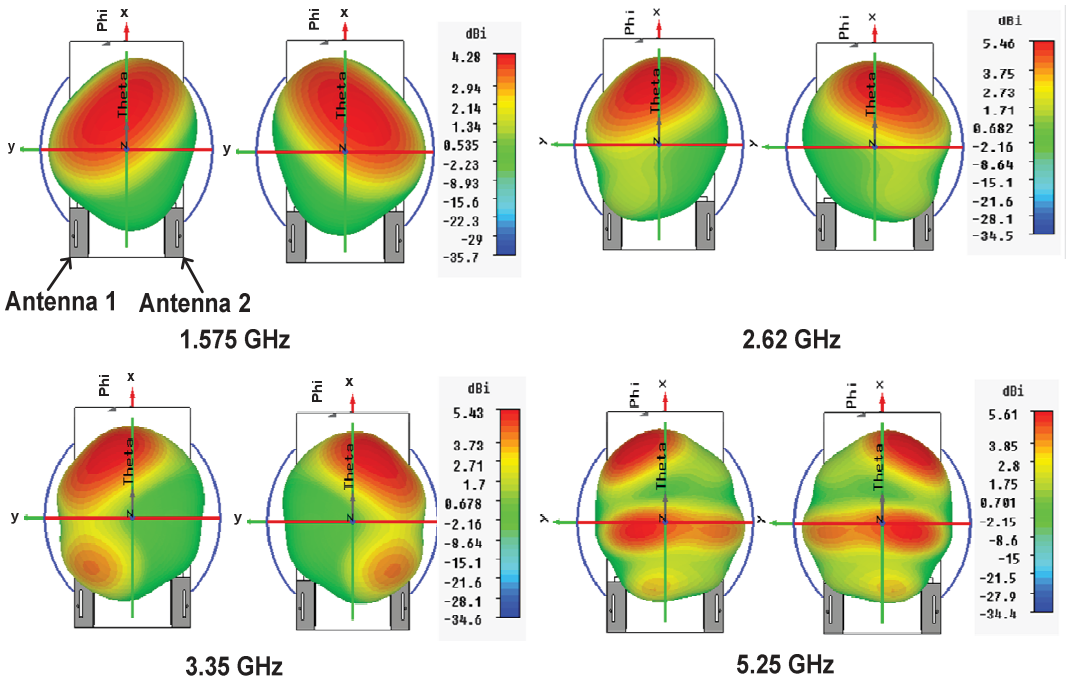

(a)

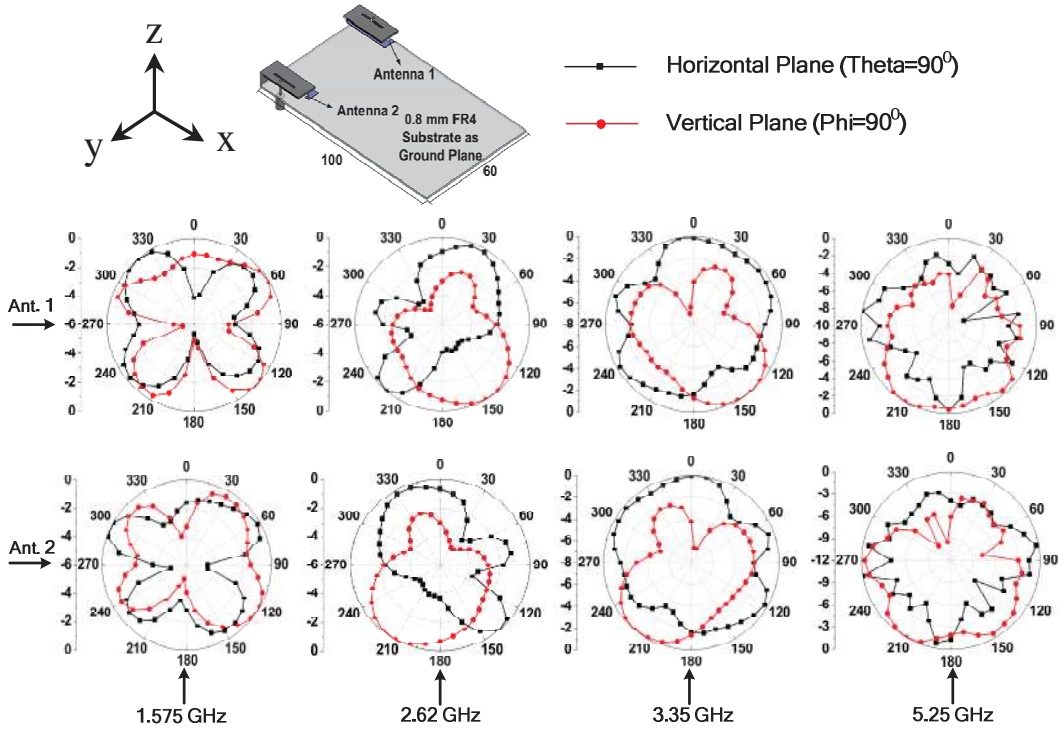

(b)

Figure 5.9: (a) Simulated 3D far field radiation patterns for the MIMO antenna at 1.575 GHz, 2.62 GHz, 3.35 GHz, and 5.25 GHz and (b) Measured 2D far field radiation patterns at 1.575 GHz, 2.62 GHz, 3.35 GHz, and 5.25 GHz.

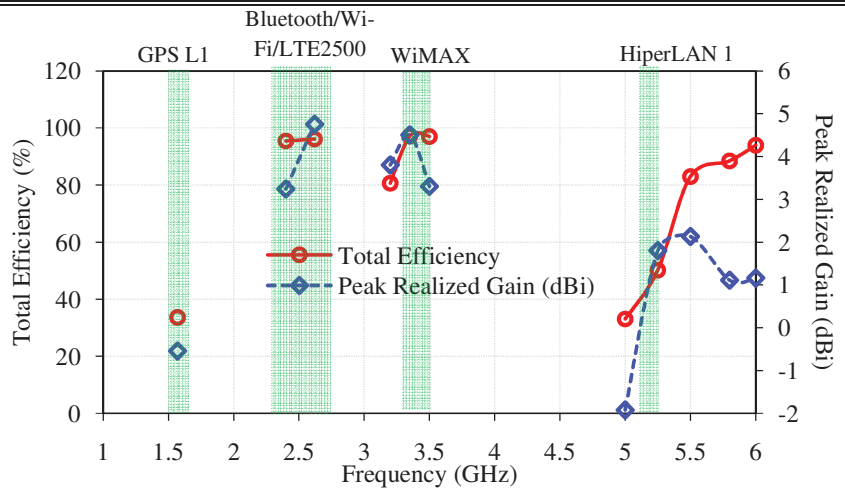

Figure 5.10: Variations of measured peak realized gain and total efficiency with frequency.

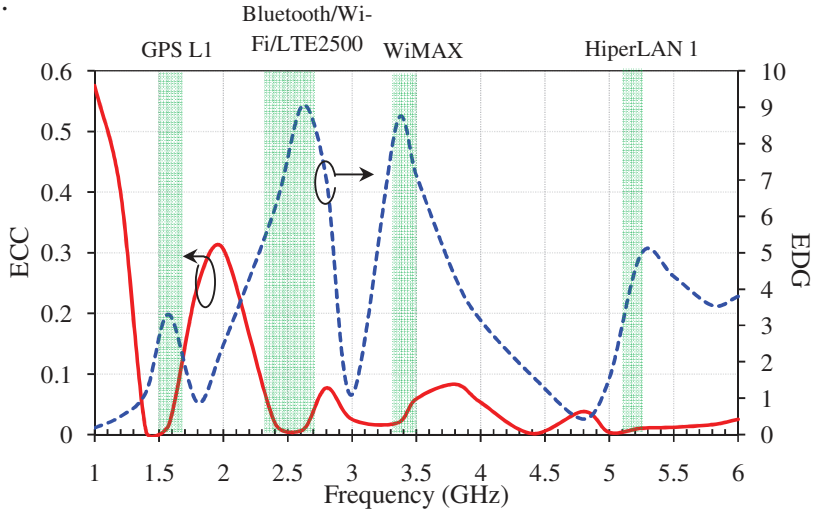

Figure 5.11: Variation of ECC and EDG with frequency.

5.3.2.2 Mean Effective Gain (MEG)

The MEG of the proposed antenna is calculated by using Eq. (2.4) which is given as [Taga (1990)]:

$$MEG = \int_0^{2\pi}\int_0^{\pi}\left[\frac{XPR}{1+XPR}G_\theta(\theta,\phi)P_\theta(\theta,\phi) + \frac{1}{1+XPR}G_\phi(\theta,\phi)P_\phi(\theta,\phi)\right] sin\theta d\theta d\phi$$

Table 5.2 gives the computed MEG for different *XPR* at different frequency bands by setting, m_v=10^0, m_H=10^0, σ_v=15^0, and σ_H=15^0. By observing the table it is clearly seen that the ratio of MEG1/MEG2 is nearly equal to unity and it indicates that the MIMO system provide the good diversity performance.

Table 5.2: MEG in free space at different frequencies

Frequency (GHz)	Indoor (XPR=5 dB)		Outdoor (XPR=1 dB)		Isotropic (XPR=0 dB)	
	MEG1	MEG2	MEG1	MEG2	MEG1	MEG2
1.575	-10.43	-10.43	-9.37	-9.37	-9.11	-9.11
2.62	-5.17	-5.18	-4.76	-4.77	-4.65	-4.66
3.35	-4.57	-4.56	-4.48	-4.48	-4.45	-4.44
5.25	-7.22	-7.20	-7.30	-7.30	-7.32	-7.33

5.3.2.3 Effective Diversity Gain (EDG)

The effectiveness of diversity is given in terms of diversity gain. Diversity gain is calculated using Eq. 2.19 [Schwartz (1965)].

$$\text{DG}= 10\sqrt{1-|\text{ECC}|^2}$$

The apparent diversity gain which is based on selection combining with respect to 1% distribution level does not include the antenna radiation efficiency. To achieve effectiveness of diversity capability antenna radiation efficiency should be considered. The EDG is calculated and are shown in Fig. 5.11.

5.4 Performances Study of Quad-Band MIMO Antenna in User Proximity with Mobile Environment

5.4.1 Simulation Setup and Configurations

The antenna characterization in free space configuration of quad-band PIFA has been discussed in the above sections. All the dimensions are clearly elaborated in the previous sections and results are also well presented in free space. To see the effect of the user proximity and actual mobile environment on the antenna performances. The antenna is considered in the actual mobile environment with mobile phone components present near to the antenna elements. As mentioned earlier, a smart phone has a number of components besides system circuit board. Fig. 5.12 shows the configuration of typical mobile phone with MIMO configuration of quad-band PIFA. In the centre of MIMO antenna elements, there is a camera whose diameter is 8.5 mm, and its thickness is 6 mm. Opposite to the

camera there is a speaker with the dimensions of 10 mm length and 8.5 mm width, respectively. A large-size touch screen LCD with volume $73 \times 47 \times 2$ mm^3 and a battery with volume $65 \times 47 \times 3$ mm^3 are located parallel with a spacing of 1 mm from the circuit board and are connected to the main circuit board via connectors. All these components are considered as Perfect Electric Conductor (PEC) during the simulation. One microphone is also accounted and it is located far from the antenna elements. A plastic box, which has a relative permittivity of 3, loss tangent of 0.06, and conductivity of 0.24 S/m, is assumed to form the housing of the mobile phone. The simulation setup of mobile environment is created in CST MWS.

Further, user body is placed near to the mobile phone (antenna with mobile environment) and position of complete mobile phone and user body [SAM head and PDA hand (Talk mode); PDA hand (Data mode)] is in accordance with the Cellular Telecommunication Industry Association (CTIA) [CTIA Report (2011)]. Generally, users use the mobile phone in three different modes i.e. Talk mode, Data mode, and Dual hand (Read mode). For the case of dual hands, since there is no standard yet, the whole antenna array and dual hands are arranged in a common handsets-holding way. The dielectric properties of the human head and hand tissue can be found in [CTIA (2011)] and given in Table 5.3. Since the antenna elements are placed symmetrically on the mobile circuit board, using the left or right hand will not cause any difference. In the simulation, we assume that the user uses the right hand (as most people do). In order to study the effect of antenna location on mobile circuit board, we consider two different locations over mobile circuit board i.e. top and bottom for each case of user proximity. We refer to the antenna close to the ear as top antenna and the one close to the mouth as bottom antenna.

All the simulation setups for the study of user proximity are created in CST MWS. The tissue model and antenna with mobile phone configuration in Talk mode are shown in Fig. 5.13(a). In Fig. 5.13(b), the tissue model and antenna locations are presented for the Data mode. The hand model and holding rules are exactly the same as in the Talk mode. The Read mode is shown in Fig. 5.13(c).

The effects of talk mode, data mode, and read mode on antenna performances are studied for top as well as bottom located MIMO antenna elements. To check the effect of user proximity on performances of PIFA, *S*-parameters, total antenna efficiency, ECC, multiplexing efficiency, MEG, TRP, and SAR are studied.

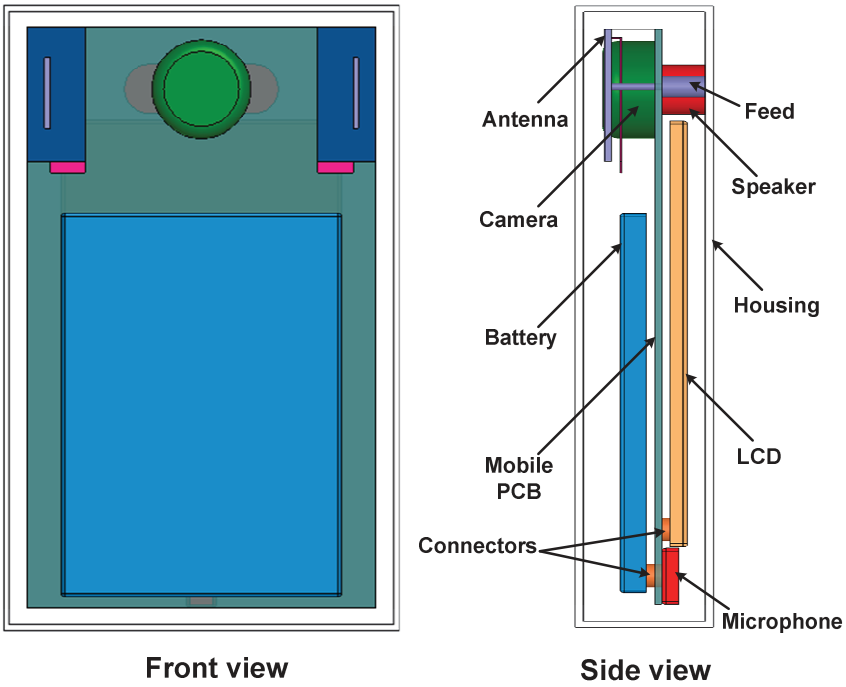

Figure 5.12: Mobile phone configuration with antenna elements.

Table 5.3: Dielectric properties of the human head and hand tissues

Frequency (GHz)	Human Head Tissue		Human Hand Tissue	
	ε	σ (S/m)	ε	σ (S/m)
1.6	40.25	1.3	27.5	0.9
2.7	38.85	2.1	25.25	1.46
3.5	37.95	2.9	24.15	1.89
5.2	36	4.65	22	2.98

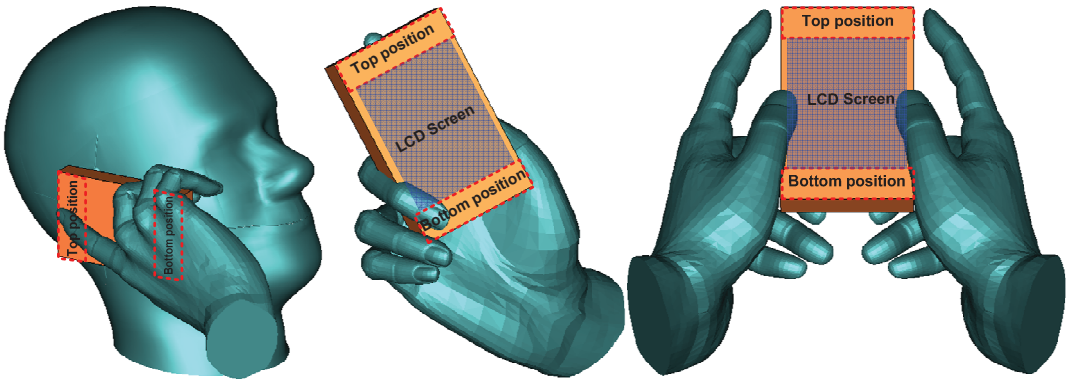

SAM head and PDA hand (Talk mode) | PDA hand (Data mode) | Dual hand (Read mode)

(a) (b) (c)

Figure 5.13: Model of antenna elements locations of (a) SAM Head and PDA Hand (Talk mode), (b) PDA Hand (Data mode), and (c) Dual Hand (Read mode).

5.4.2 *S*-parameters Analysis

In the free space, the quad-band PIFA is designed and tested successfully for the operating bands of GPS L1 (1.565-1.585 GHz), Bluetooth/Wi-Fi (2.4-2.484 GHz), LTE2500 (2.5-2.57 GHz for uplink, 2.62-2.69 GHz for downlink), WiMAX (3.3-3.4 GHz), and HiperLAN1 (5.15-5.35 GHz) and results are shown in Fig. 5.8. Further, antenna is placed in actual mobile environment to study the effect of near field mobile environment and the variations of *S*-parameters are shown in Fig. 5.14. It is observed that band 2 and 3 (Bluetooth/ Wi-Fi, LTE2500, and WiMAX application bands) shifted towards lower frequency side but still antenna provides aforesaid operating bands in the mobile environment based on the 6dB return loss and isolation between antenna elements is also well below -12 dB.

In order to verify the robustness of the antenna performances with user proximity, initially *S*-parameters are studied for two different positions of the antenna on mobile circuit board i.e. antenna on the top position and bottom position. In the case of Talk mode, variations of *S*-parameters are shown in Fig. 5.15(a). It is observed that, when antenna is located at the bottom of the mobile circuit board the reflection coefficient of Ant. 2 is disturbed due to which antenna

does not cover the desired operating bands properly. This is happened due to the large reflection from human head. Top located MIMO antenna provides good impedance matching and operating bandwidth. While in the case of data and read mode, top as well as bottom located MIMO antenna provides good impedance matching because the antenna coverage by users body is less as compared to the talk mode, resulting in less reflection losses and antenna provides above mentioned operating bands and the variations of *S*-parameters for the data mode and read mode are shown in Fig. 5.15(b) and Fig. 5.15(c), respectively.

5.4.3 Analysis of Antenna Performance in Different Configurations

In this section, the performance parameters i.e., total efficiency, ECC, multiplexing efficiency (ME), and mean effective gain (MEG) are investigated for three different configuration namely, talk mode, data mode, and read mode to test the characteristics of PIFA. The total antenna efficiency is calculated by considering the mismatch losses [Balanis (2005)]. In addition to this, all the ECC results are calculated through 3D far field radiation patterns for which formulae has been discussed in Chapter 2.

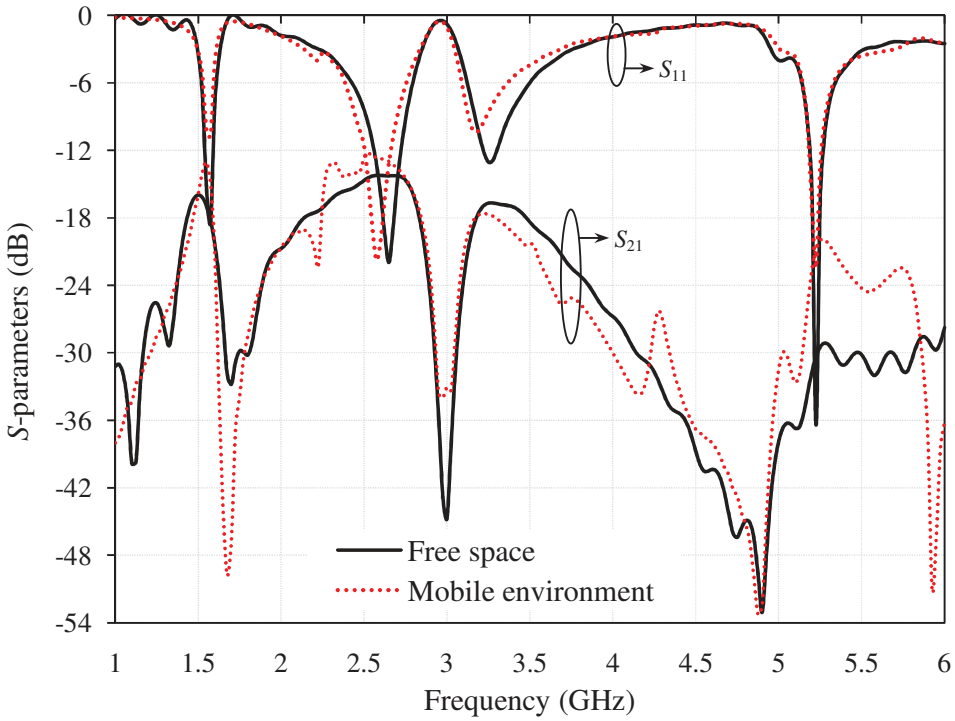

Figure 5.14: Variation of *S*-parameters in mobile environment.

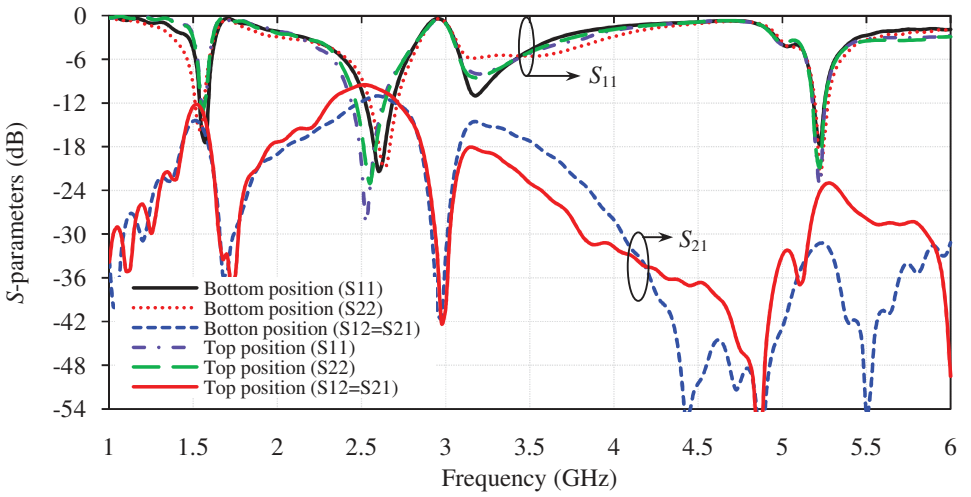

(a)

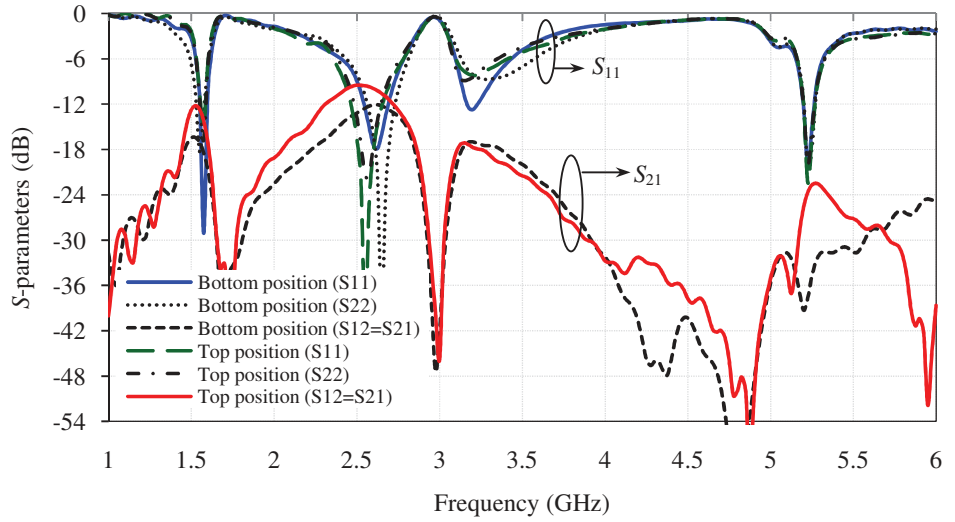

(b)

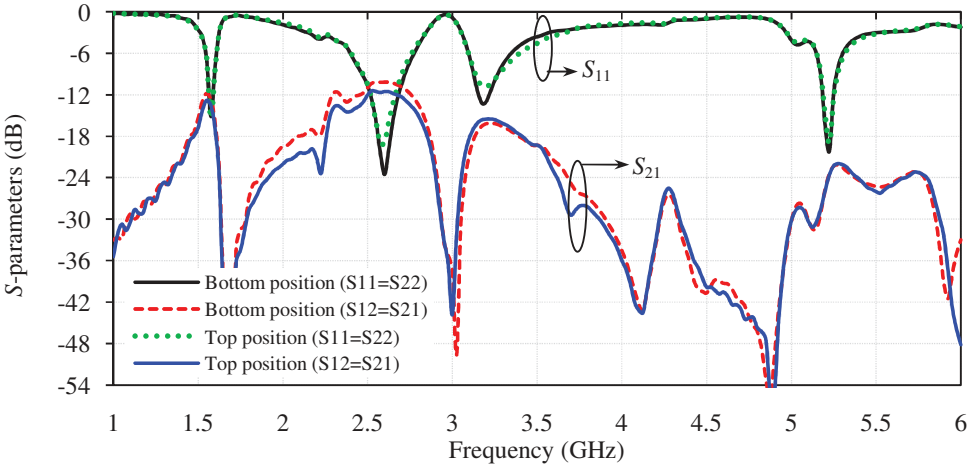

(c)

Figure 5.15: Variation of *S*-parameters of PIFA in the presence of user proximity (a) Talk mode, (b) Data mode, and (c) Read mode.

Further, multiplexing efficiency (ME) is introduced in order to estimate the MIMO channel performance simply through the efficiency and envelope correlation coefficient of the MIMO antenna elements. This formula is based on high SNR and isotropic environment, and can be found in [Tian *et al.* (2011)] and also, given in Chapter 2.

Next parameter, mean effective gain (MEG) is considered for the study of effect of user proximity on antenna performance. MEG gives the statistical measure of antenna gain in a given mobile environment. The MEG defined as the ratio between the mean received power of antennas over a random route, and the total mean incident power at the antenna elements. In order to calculate the MEG of a particular antenna element the expression is given in [Taga (1990)]. The conditions that have been elaborated in Chapter 2 are considered here for MEG calculation.

5.4.3.1 SAM Head and PDA Hand (Talk Mode)

The total efficiency of each port for top and bottom located antenna elements are calculated and shown in Fig. 5.16(a). It is observed that when antennas are mounted on the top of the mobile circuit board efficiency is more as compared to the bottom position. This is because of the bottom part of the thumb or tip of the little finger is near to the bottom located antenna elements. The efficiency at GPS L1 band is more than 10% whereas for the other higher operating bands it is more than 25%. In the case of bottom position, efficiency is low as compared to the top located antennas over the entire operating bands.

By utilizing the formula of ECC which is based on far field data, ECC is calculated and shown in Fig. 5.16(b). The correlation for bottom located MIMO elements is slightly higher than the top location. This is mainly due to the entire MIMO antenna system covered by large human. However, the ECC is well below 0.5 over the entire operating band for both cases.

The multiplexing efficiency of different antenna elements are calculated and shown in Fig. 5.16(c). As expected, due to higher efficiency and lower correlation, the top located antenna elements have better multiplexing efficiency than the other combination of the antennas.

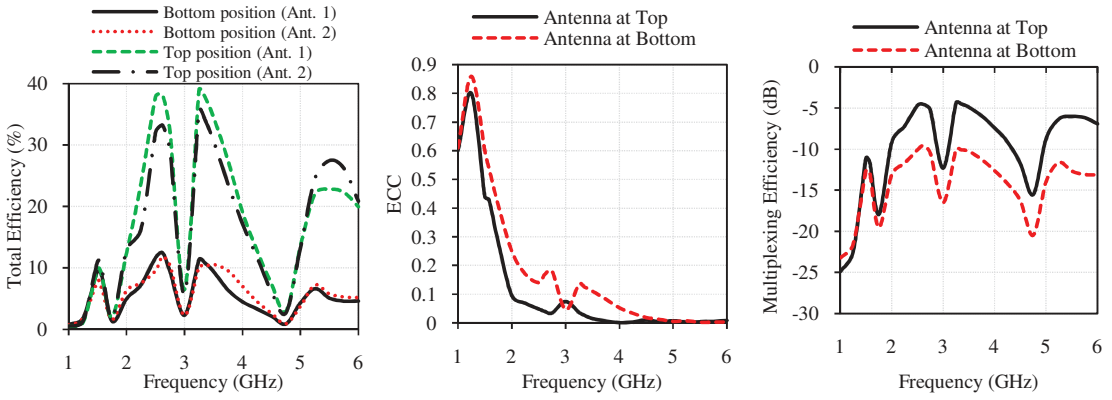

(a) (b) (c)

Figure 5.16: (a) Total efficiency, (b) ECC, and (c) Multiplexing efficiency of the SAM Head and PDA Hand (Talk mode) for PIFA.

The computed values of the MEG are given in the Table 5.4. It is observed that the drop of the MEG values for the bottom antennas is slightly more than the top located antennas. At the GPS L1 band the drop in MEG is about 6 dB, at 2.62 GHz and 3.35 GHz the drop in MEG is approximately 1 dB to 2 dB respectively, and at 5.25 GHz the drop is nearly 5 dB as compared to the free space MEGs. The change of the MEG at different port in user proximity is due to the asymmetrical user body coverage around the antenna elements. However, the ratio of MEG is nearly close to unity, which satisfies the equality criterion for the MIMO antenna systems.

5.4.3.2 PDA Hand (Data Mode)

The total efficiency for the data mode is shown in Fig. 5.17(a). It is observed that, in the case of bottom position of the antenna, the efficiency difference for each ports is not as significance as that in the case of top position. Also, efficiency difference between all the ports is less significant than the Talk mode. In other words, the SAM head causes larger effects for the bottom located antenna elements. One can observe that at GPS L1 band, the total efficiency of antenna is somewhat smaller than the efficiency of the other bands.

The correlation coefficient is shown in Fig. 5.17(b). It is observed that the correlation of top located antenna elements has the lowest correlation and its

characteristics are same as in Talk mode but the values are lower than that of the Talk mode.

The multiplexing efficiency is shown in the Fig. 5.17(c). It is observed that in the GPS L1 band, due to almost same total efficiency for top as well as bottom located antenna, the multiplexing efficiency is almost same. But for the other operating bands, the bottom position of the antenna brings lower multiplexing efficiency because of the lower total efficiency and higher correlation between the MIMO antenna elements.

However, the variation of MEG for data mode is approximately same as the variation of MEG for talk mode and also ratio is close to unity which satisfies the diversity criteria. The values are given in Table 5.4.

5.4.3.3 Dual Hand (Read Mode)

The variations of total efficiency for read mode is shown in Fig. 5.18(a). The variation of total efficiency between each antenna elements for top as well as bottom location is quite small in comparison to the Talk mode and Data mode. But the bottom position of the antenna over mobile circuit board gives lower efficiency than the top position of the antenna at 2.62 GHz, 3.35 GHz and 5.25 GHz bands. However, the total efficiency is larger than the previous two cases and this is because of the less user hand coverage.

The calculated values of ECC are shown in Fig. 5.18(b). It is observed that the value of ECC is almost equal for top as well as bottom located MIMO antenna. This is due to the symmetrical placement of the hand around the antenna elements.

In the Read mode, due to the almost similar correlation between antenna elements, the total efficiency plays significant role to decide the multiplexing efficiency. As can be observed that the lower total efficiency at higher frequency bands for bottom position of the MIMO antenna elements provide the lower multiplexing efficiency as shown in Fig. 5.18(c).

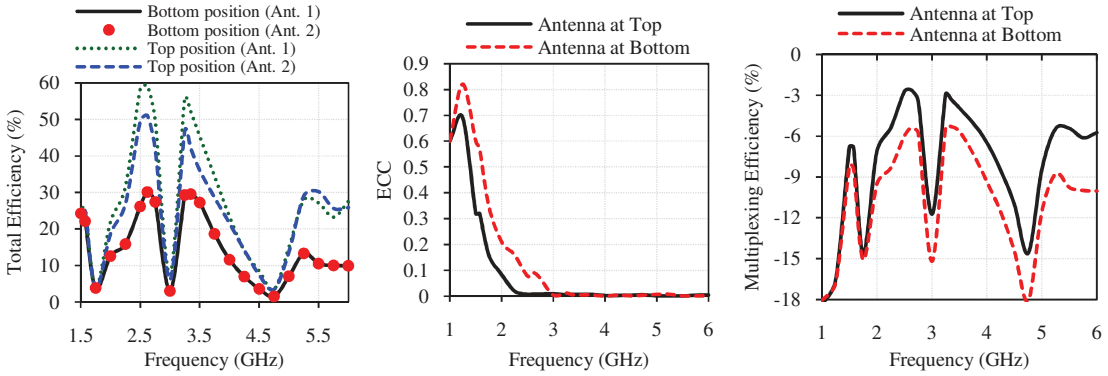

(a) (b) (c)

Figure 5.17: (a) Total efficiency, (b) ECC, and (c) Multiplexing efficiency of the PDA Hand (Data mode) for PIFA.

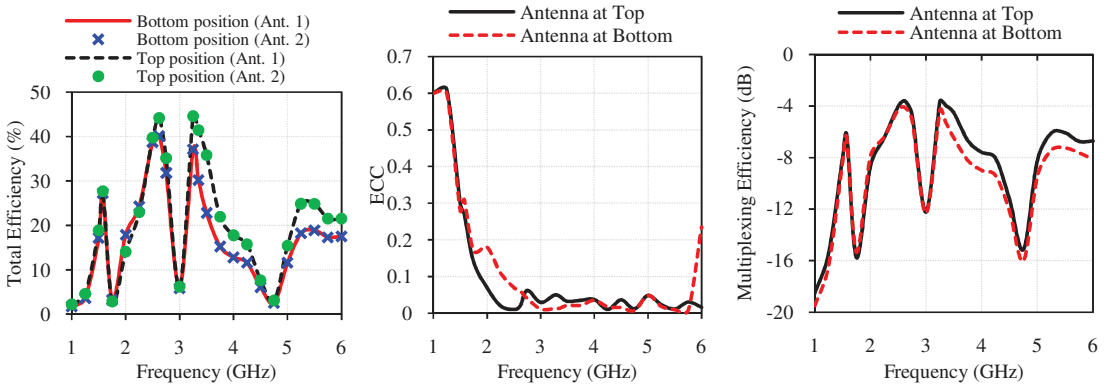

(a) (b) (c)

Figure 5.18: (a) Total efficiency, (b) ECC, and (c) Multiplexing efficiency of the Dual Hand (Read mode) for PIFA.

From the Table 5.4, it is observed that at the GPS L1 band the drop of MEG is around 7dB for top as well as bottom located antenna whereas the variation of the MEG for other bands is similar in the two modes i.e. Talk mode and Data mode.

5.4.4 Total Radiated Power (TRP) Analysis

The TRP is defined as that correlate the field performance of the antenna and is influenced by the transmission power and the antenna efficiency. The TRP can be defined as [CTIA (2005)],

$$TRP\ (W) = Conducted\ Power\ (W) \times E_{miss} \times E_{rad} \qquad (5.2)$$

where, E_{miss} and E_{rad} are the mismatch and radiation efficiency of antenna respectively, the conducted power is the transmitted power. In this study, the conducted power is normalized to 1 W or 30 dBm. In the case of multi element MIMO system, the TRP is calculated for each element of MIMO antenna system and named as TRP1 and TRP2 for Ant. 1 and Ant. 2, respectively for top and bottom location of the antenna elements over mobile circuit board. The TRPs are calculated for above three cases namely, Talk mode, Data mode, and Read mode including free space are given in Table 5.5. It is ascertained that in the case of free space, TRP of Ant. 1 and Ant. 2 are same due to the uniform environment around the MIMO antenna elements. However, due to the low reflection loss and high total efficiency, the TRPs in free space is high i.e. more than 22 dBm. When proposed antenna is implemented in real scenario of talk mode, data mode, and read mode, the TRP decreases. For the bottom position, lower TRP is observed because of the larger body coverage and absorption of the power in head and hand phantom.

Table 5.4: Variations of MEG in different user proximity for PIFA

Frequency (GHz)		Antenna at Top		Antenna at Bottom	
		MEG 1	MEG 2	MEG 1	MEG 2
1.575	Free space	-9.7	-9.7	-9.7	-9.7
	Talk mode	-3.6	-3.6	-3.1	-3.1
	Data mode	-3.1	-3.5	-3.2	-4
	Read mode	-2.8	-2.82	-2.6	-2.58
2.62	Free space	-5.3	-5.3	-5.3	-5.3
	Talk mode	-4.7	-4.2	-3	-3.5
	Data mode	-3.5	-3.8	-3.9	-3.8
	Read mode	-4.3	-4.26	-4.5	-4.52
3.35	Free space	-5.1	-5.1	-5.1	-5.1
	Talk mode	-4.4	-3.25	-2.35	-1.8
	Data mode	-3.3	-3.5	-4.2	-4.3
	Read mode	-3.5	-3.5	-3.1	-3
5.25	Free space	-7.9	-7.9	-7.9	-7.9
	Talk mode	-2.9	-2.16	-2.15	-3.8
	Data mode	-3.4	-3.5	-3	-3.9
	Read mode	-4.2	-4.16	-3.5	-3.54

Further, to understand the power loss in presence of user proximity compared to the free space, bar chart is given at different frequencies for each of the position (Top and Bottom position) in Fig. 5.19. It is observed that the power loss at lower frequency (GPS L1 band) is 6dB and 8dB for top position and bottom position, respectively. The power loss for each antenna elements is slightly different because the presence of user around each antenna element is not symmetrical. So this asymmetrical coverage of the user body brings different radiation losses for each antenna elements for top as well bottom position. It is also observed that the bottom position of the antenna elements suffer from more radiation losses in comparison to the top located antenna. Each antenna element for both the positions and also at each frequencies has same power loss and this is due to the same environment around each antenna elements. The ranking of the power loss at all the frequencies in the user proximity is approximately Talk mode, Data mode, and Read mode.

Table 5.5: Variations of TRP in different user proximity for PIFA

Frequency (GHz)		Antenna at Top		Antenna at Bottom	
		TRP 1	TRP 2	TRP 1	TRP 2
1.575	Free space	22	22	22	22
	Talk mode	16.3	16.8	16.4	15
	Data mode	21.8	20.9	18.8	20.4
	Read mode	21.4	21.4	21.33	21.34
2.62	Free space	26.6	26.6	26.6	26.6
	Talk mode	22.8	22.2	17.9	17.7
	Data mode	24.7	24.1	21.4	21.8
	Read mode	23.4	23.4	23	23
3.35	Free space	26.3	26.3	26.3	26.3
	Talk mode	22.7	22.3	17.3	17
	Data mode	24.8	23.2	19.8	21.6
	Read mode	23.2	23.2	21.7	21.7
5.25	Free space	24.1	24.1	24.1	24.1
	Talk mode	20.4	20.9	15.2	15.5
	Data mode	21.4	21.6	15.2	18.2
	Read mode	20.9	20.9	19.6	19.6

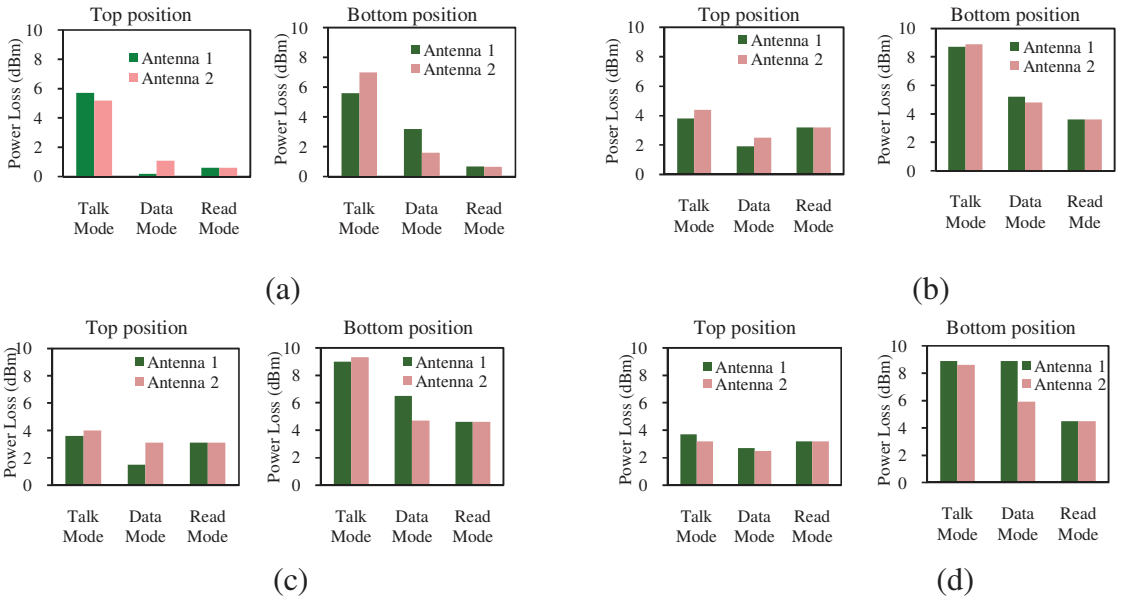

Figure 5.19: Variations of power loss in user proximity at different frequencies for PIFA at (a) 1.575 GHz, (b) 2.62 GHz, (c) 3.35 GHz, and (d) 5.25 GHz.

5.4.5 Specific Absorption Rate (SAR) Analysis

The SAR values of Ant. 1 and Ant. 2 are investigated according to the CTIA standard [CTIA (2005)] (SAM head and cheek touch) and setup is shown in Fig. 5.20. The American standard (FCC) postulate 1.6 W/kg SAR averaged over 1g tissues, while the European standard postulate 2 W/kg SAR averaged over 10g tissues. The SAR values for top and bottom located antenna is calculated and given in Table 5.6. It is observed that the top located antenna is having larger SAR values as compared to the bottom located antenna because of the distance difference between antenna and head phantom. The top located antenna is exaclty at 5mm distance from the head phantom whereas bottom located antenna is having larger distance from human head phantom as compared to the top located antenna. It is also observed that the SAR is less for both the standard because the antenna is covered by the plastic box. It can also be observed that for both the positions, SAR values of Ant. 1 and Ant. 2 are somewhat different because human head phantom is not planar. But from the table, it can be concluded that for both the positions, values of SAR satisfies the criteria of FCC and European standard.

Further, when the dual antenna operates simultaneously, the value of SAR to PEAK Location Spacing Ratio (SPLSR) is utilized to evaluate the SAR

performance [FCC Report (2008)]. In the calculation of SPLSR, the SAR1 and SAR2 are related to Antenna 1 and Antenna 2, respectively. The separation distance of the two SAR peaks and values of SAR are calculated using CST MWS simulation software. The calculation of SAR is averaged over 1g and 10g average human tissue. The SPLSR is calculated at four different resonating frequencies i.e. 1.575 GHz, 2.62GHz, 3.35 GHz, and 5.25 GHz. The testing power for SAR calculation is 21dBm for 2.45GHz and 3.5GHz and 17dBm for 5.8GHz [CTIA Report (2005)]. The calculated values of SPLSR are given Table 5.7. It is observed that the calculated values of SPLSR are well below the limits defined by FCC i.e. 0.3 for top as well as bottom located MIMO antenna. However, bottom located MIMO configuration shows lower SPLSR than top located configuration due to the larger distance between antenna and human cheek for bottom position.

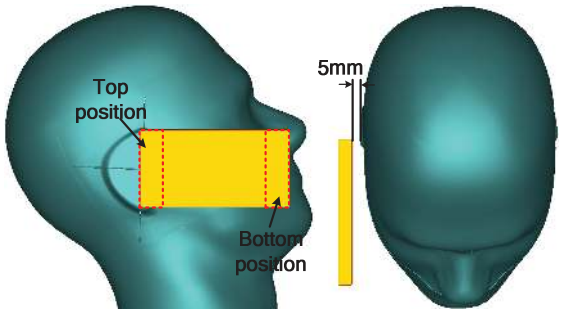

Figure 5.20: SAR simulation setup according to CTIA.

Table 5.6: SAR values on head phantom due to PIFA.

Top Position					
Antenna ↓ / Frequency →		1.575 GHz	2.62 GHz	3.35 GHz	5.25 GHz
Ant. 1 (W/kg)	FCC	0.319	0.399	0.356	0.258
	European	0.206	0.207	0.163	0.1
Ant. 2 (W/kg)	FCC	0.383	0.396	0.56	0.168
	European	0.222	0.220	0.222	0.065
Bottom Position					
Ant. 1 (W/kg)	FCC	0.237	0.403	0.267	0.121
	European	0.164	0.222	0.137	0.051
Ant. 2 (W/kg)	FCC	0.282	0.432	0.419	0.161
	European	0.173	0.243	0.191	0.064

Table 5.7: Calculated values of SPLSR of quad-band MIMO antenna

Top Position								
Distribution of SAR over 1-g tissue					Distribution of SAR over 10-g tissue			
Freq. (GHz)	SAR_1 (W/kg)	SAR_2 (W/kg)	Separation distance b/w SAR peaks (D) unit in centimetre (cm)	SPLSR $=\frac{(SAR_1+SAR_2)}{D}$ (W/kg/cm)	SAR_1 (W/kg)	SAR_2 (W/kg)	Separation distance b/w SAR peaks (D) unit in centimeter (cm)	SPLSR $=\frac{(SAR_1+SAR_2)}{D}$ (W/kg/cm)
1.575	0.319	0.383	2.2	0.3	0.206	0.222	2.2	0.19
2.62	0.399	0.396	2.7	0.29	0.207	0.220	1.6	0.27
3.35	0.356	0.56	4.12	0.22	0.163	0.222	4	0.096
5.25	0.258	0.168	6.1	0.07	0.1	0.065	5.2	0.032
Bottom Position								
1.575	0.237	0.282	3.7	0.14	0.164	0.173	1.6	0.21
2.62	0.403	0.432	5.6	0.15	0.222	0.243	1.92	0.24
3.35	0.262	0.419	5.8	0.12	0.137	0.191	5.8	0.06
5.25	0.121	0.161	8.08	0.035	0.051	0.064	7.4	0.02

5.5 Summary

A quad-band MIMO antenna covering GPS L1 band along with Bluetooth/ LTE2500/ WiMAX/ HiperLAN1 has been elaborated for next generation (4G) mobile phone application in this chapter. The proposed antenna is having small and compact structure that can easily be fitted inside the mobile device. An extra resonating arm is added into the structure at an appropriate position to convert unwanted bandwidth into the desired one. Owing to the greater separation between the two antenna elements over the ground plane, the proposed antenna is having good isolation characteristics even in the absence of any isolation improvement technique. Finally, optimized MIMO antenna is fabricated and measured with the help of performance network analyzer and experimental results are in close agreement with the simulated one. Good pattern diversity is obtained through the proposed antenna that is suitable for mobile communication by mitigating the multipath fading. To check the robustness of the proposed antenna,

three commonly used configurations namely, Talk mode, Data mode, and Read mode are considered by placing the antenna at top as well as bottom of the mobile circuit board. For all these configurations diversity parameters and MIMO parameters are calculated. From the above discussed results, it is revealed that the top located MIMO antenna element shows better performances than bottom located antenna. In the presence of user body near to the MIMO antenna power loss is observed as compared to the free space. It is observed that the bottom position shows higher loss as compared to the top position. The calculated values of SPLSR are found well below the defined limit of 0.3 for both the position (top position and bottom position).

After the completion of detail analysis of quad-band PIFA with MIMO configuration in both free space as well as actual mobile environment with user proximity, the analysis of slim, printed monopole MIMO/Diversity antenna is taken up in the next chapter i.e., chapter six.